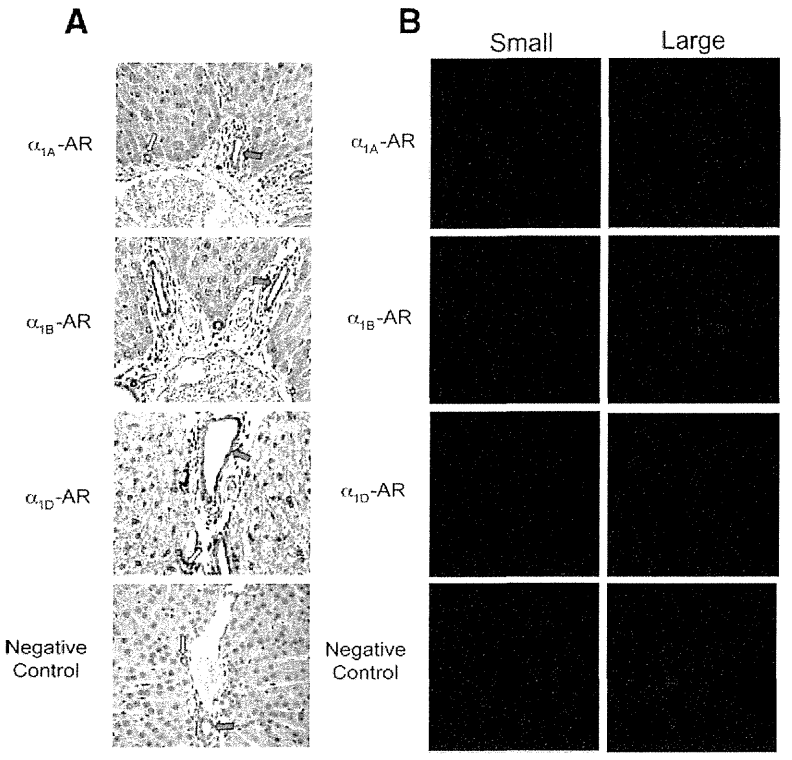

Fig. 1. Expression of α_{1A}, α_{1B}, α_{1D} AR by immunohistochemistry (A) in liver sections, and immunofluorescence (B) in immortalized small and large cholangiocytes. (A) Small (yellow arrows) and large (red arrows) bile ducts were positive for α_{1A}-, α_{1B}-, and α_{1D}-AR expression. Original magnification, ×20. (B) Immortalized small and large cholangiocytes were positive for α_{1A}-, α_{1B}-, and α_{1D}-AR. AR expression is shown in red with nuclei counterstained with DAPI (4′,6-diamidino-2-phenylindole; blue). Original magnification, ×60. The negative control performed without the primary antibody is presented at the bottom of the figure. Bile ducts (A) and immortalized small and large cholangiocytes (B) express α_{1A}, α_{1B}, and α_{1D}-AR.

cholangiocytes (Fig. 4A). To determine the potential role of each of the AR subtypes on the proliferation of immortalized small and large cholangiocytes, we performed MTS proliferation assays in the presence/absence of α_1 (phenylephrine), α_2 (UK14,304), β_1 (dobutamine), β_2 (clenbuterol) or β_3 (BRL 37344) AR agonists. In large cholangiocytes, we observed that dobutamine, clenbuterol, and BRL 37344 stimulated proliferation, whereas phenylephrine and UK14,304 had no effect on the growth of large cholangiocytes (Fig. 4B). In addition to phenylephrine, dobutamine (but not clenbuterol, and BRL 37344) increased small cholangiocyte proliferation (Fig. 4B). Because activation of β-adrenergic receptors regulates biliary functions by increased intracellular cAMP levels in cholangiocytes,[9] we focused our studies on the role of phenylephrine (an α_1-AR agonist stimulating IP_3/Ca^{2+} levels)[10,34] on Ca^{2+}-dependent signaling in small cholangiocytes. We demonstrated that α_{1A} (RS17053), α_{1B} (Rec15/2615) and α_{1D} (BMY7378) AR antagonists induced a partial yet significant reduction in phenylephrine-induced proliferation of immortalized small cholangiocytes (Fig. 4C). However, levels of proliferation stimulated by phenylephrine in the presence of the antagonists remain significant in comparison to basal control proliferation, which demonstrates that all three receptor subtypes are involved in phenylephrine-induced proliferation (Fig. 4C).

Phenylephrine Stimulates the Proliferation of Immortalized Small Cholangiocytes Via Ca2+-Dependent Signaling Mechanism. Phenylephrine increased intracellular IP_3 (but not cAMP, not shown) levels (basal: 0.39 ± 0.03 versus phenylephrine: 0.62 ± 0.07 pmol/1 × 10^7 cells; $P < 0.01$) in immortalized small cholangiocytes. Phenylephrine-stimulated proliferation of immortalized small cholangiocytes was blocked by BAPTA/AM, CAI,[4] 11R-VIVIT, and MiA (Fig. 4D).

Phenylephrine Stimulates the Nuclear Translocation of NFAT and DNA-Binding Activity of NFAT2/4 and Sp1 in Immortalized Small Cholangiocytes. To further define the role of NFAT in phenylephrine-stimulated proliferation, we performed experiments to evaluate nuclear translocation and DNA-binding activity of NFAT2 and NFAT4 in immortalized small cholangiocytes. By immunofluorescence, phenylephrine stimulates nuclear translocation of both NFAT2 and NFAT4 in small cholangiocytes (Fig. 5). This translocation that was blocked by inhibitors of upstream Ca^{2+}-dependent signaling (i.e., benoxathian [nonsubtype selective α_1-AR antagonist],[31] BAPTA/AM, and CAI) (Fig. 5), which confirms the results of the proliferation studies (Fig. 4D). The activation of NFAT and Sp1/3 DNA-binding activity was determined by EMSA and DNA-binding activity ELISA. We found by EMSA that phenylephrine stimulates time-dependent activation of NFAT

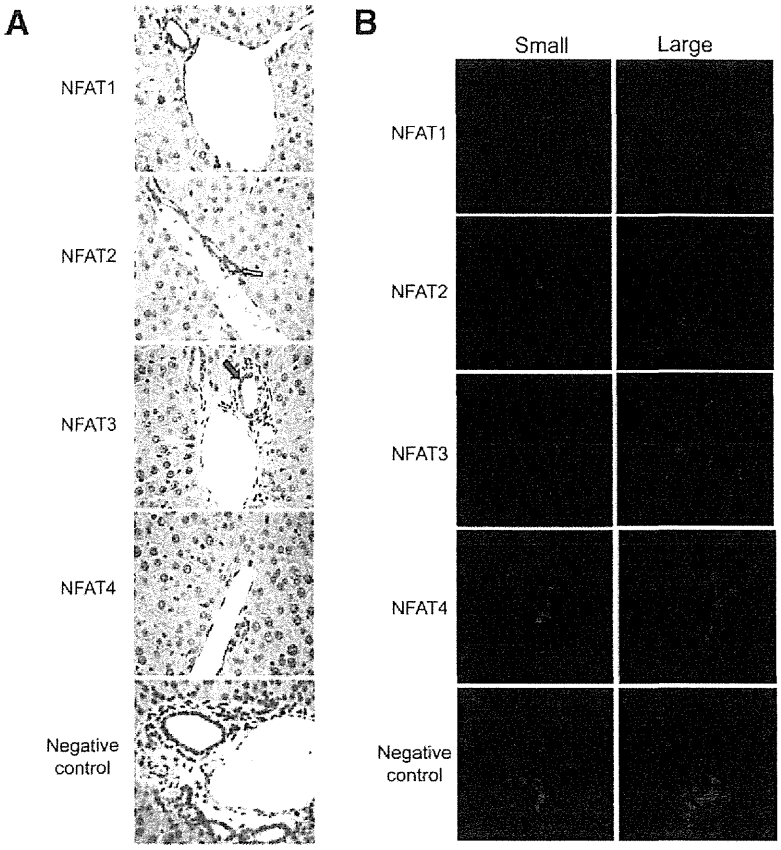

Fig. 2. Expression of NFAT isoforms by immunohistochemistry (A) in liver sections, and immunofluorescence (B) in immortalized small and large cholangiocytes. (A) NFAT2 and 4 were expressed predominantly by small bile ducts (yellow arrows; for semiquantitative data see Supporting Information Table 1). A small percent of cholangiocytes in large bile ducts (red arrows) stained positively for NFAT2 and 4. NFAT3 was expressed only in large bile ducts, whereas NFAT1 was not expressed in either sized bile ducts. Original magnification, ×20. (B) A similar expression profile was observed in immortalized small and large cholangiocytes. Small cholangiocytes were positive for NFAT2 and 4. Large cholangiocytes were positive for NFAT3, whereas neither cell type expressed NFAT1. Original magnification, ×60. A representative negative control performed without the primary antibody is presented at the bottom of the figure.

DNA-binding in small cholangiocytes (Fig. 6). The consensus sequence used in the EMSA will bind both NFAT2 and NFAT4 (elucidation of the involvement of isoforms was determined by knockdown experiments discussed later). NFAT2 DNA-binding activity was confirmed by DNA-binding activity ELISA. The ELISA kit used recognizes the specific DNA-binding activity of NFAT2 (and not other NFAT isoforms as

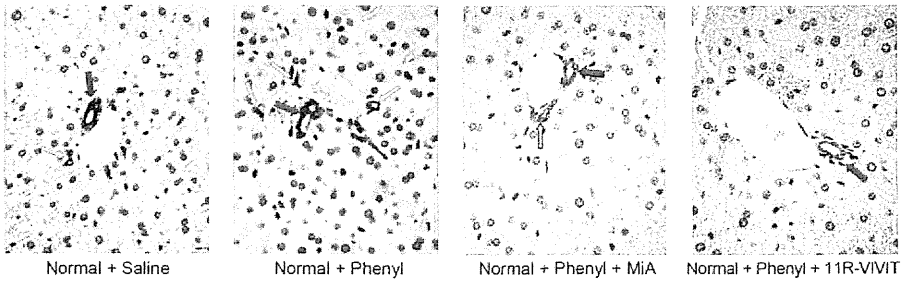

	Intrahepatic Bile Duct Mass (% surface)			
	Normal + Saline	Normal + Phenyl	Normal + Phenyl + MiA	Normal + Phenyl + 11R-VIVIT
Small Ducts	0.042 ± 0.007	0.092 ± 0.012*	0.052 ± 0.005	0.053 ± 0.004
Large Ducts	0.163 ± 0.005	0.163 ± 0.007	0.168 ± 0.009	0.167 ± 0.008

Fig. 3. Expression of CK-19 by immunohistochemistry in liver sections of normal mouse treated with vehicle or phenylephrine for 1 week in the absence or presence of 11R-VIVIT or MiA. Large (red arrow) and small (yellow arrows) ducts are indicated. Original magnification, ×40. Measurement of IBDM of small and large cholangiocytes in liver sections from the selected groups of mice. Chronic administration of phenylephrine to normal mice induces a significant increase in IBDM of small but not large cholangiocytes, increase that was blocked by 11R-VIVIT and MiA. *$P = 0.0022$ (by Mann-Whitney test) versus IBDM of small cholangiocytes from normal mice treated with phenylephrine versus normal mice treated with vehicle.

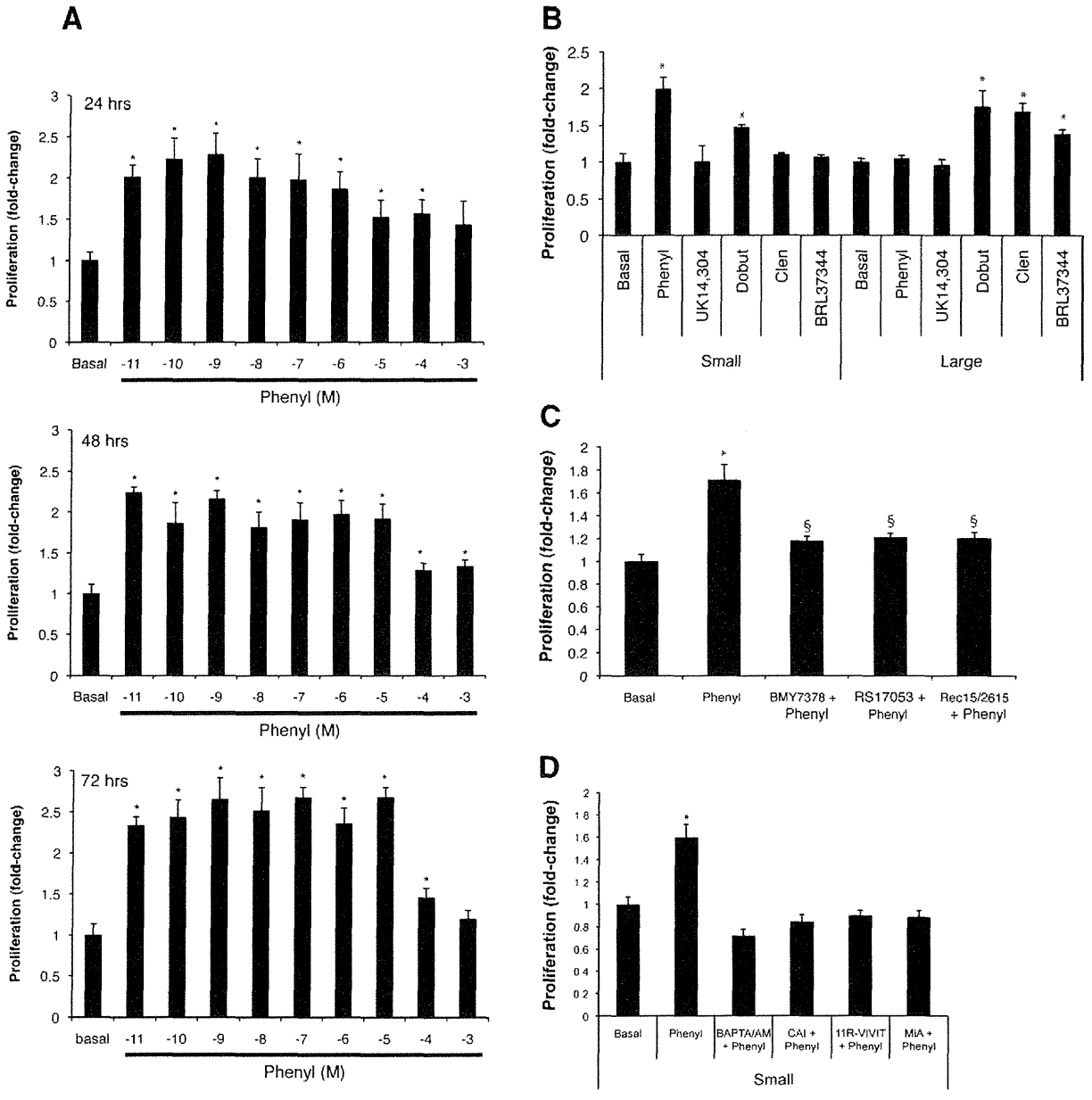

Fig. 4. (A) Effect of different doses (10^{-11} to 10^{-3} M) of phenylephrine on the proliferation of immortalized small cholangiocytes. The doses (10^{-11} to 10^{-5} M) used for phenylephrine induced a similar increase in small cholangiocyte proliferation. Asterisk (*) denotes significance ($P < 0.05$) when compared with the respective basal treatment using a Kruskal-Wallis test (n = 6-14). (B) In addition to phenylephrine, dobutamine increased small cholangiocyte proliferation. In immortalized large cholangiocytes, dobutamine, clenbuterol and BRL 37344 induced a significant increase in proliferation, whereas phenylephrine and UK14,304 had no effect. Asterisk (*) denotes significance ($P < 0.05$) when compared with the respective basal treatment using a Kruskal-Wallis test (n = 14). (C) Effect of phenylephrine (10 μM for 24 hours) on the proliferation of immortalized small cholangiocytes in the absence or presence of selective AR antagonists. α_{1A}-, α_{1B}-, and α_{1D}-AR antagonists induced a partial yet significant reduction in phenylephrine-induced small cholangiocyte proliferation. Asterisk (*) denotes significance ($P < 0.05$) when compared with the respective basal treatment using a *t* test (n = 14). Section symbol (§) denotes significance ($P < 0.05$) when compared with phenylephrine-induced proliferation. (D) Phenylephrine stimulates small cholangiocytes proliferation in a Ca^{2+}-dependent mechanism. Small mouse cholangiocytes were stimulated with phenylephrine in the presence/absence of BAPTA/AM, CAI, 11R-VIVIT, or MiA. Phenylephrine-stimulated small cholangiocyte proliferation was prevented by BAPTA/AM, CAI, 11R-VIVIT, or MiA. Asterisk (*) denotes significance ($P < 0.05$) when compared with the respective basal treatment using a Kruskal-Wallis test (n = 14).

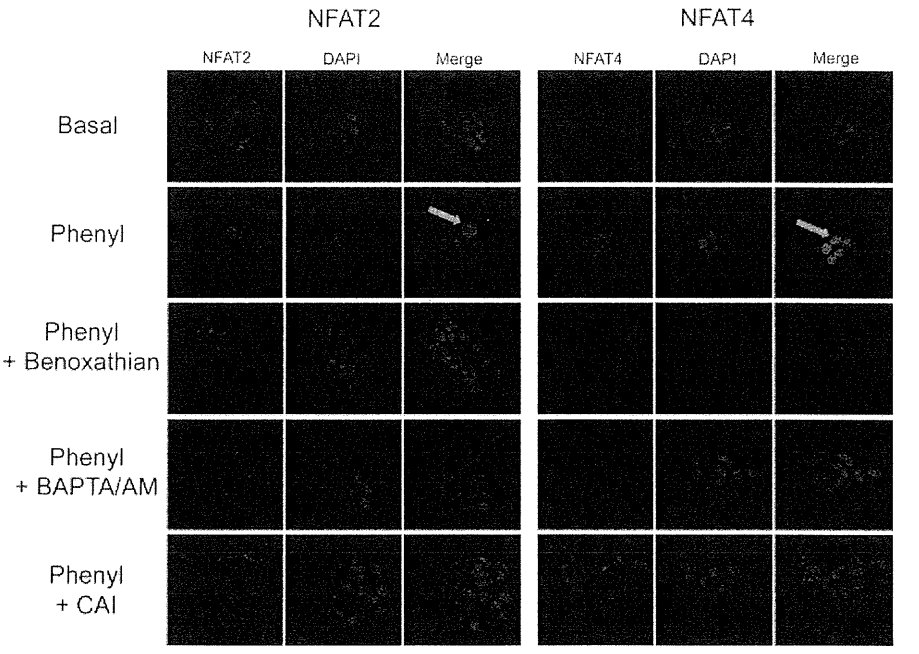

Fig. 5. Phenylephrine stimulates the nuclear translocation of NFAT2 and NFAT4. Immortalized small cholangiocytes were stimulated with phenylephrine in the presence/absence of benoxathian, BAPTA/AM, and CAI for 60 minutes. By immunofluorescence, phenylephrine stimulates the nuclear translocation of NFAT2 and NFAT4 (arrows), which was blocked by benoxathian, BAPTA/AM, and CAI. Original magnification, ×60.

there are no commercially available kits). Our results demonstrate that phenylephrine stimulates NFAT2 DNA-binding activity in small cholangiocytes, which was blocked by BAPTA/AM and CAI (Fig. 7A). We also found that phenylephrine stimulates the time-dependent increase in Sp1 DNA-binding activity in small cholangiocytes as determined by EMSA (Fig. 7B). The DNA-binding specificity of Sp1 when challenged during cold competition was determined and presented in Supporting Information Fig. 3. Because both Sp1 and Sp3 are known to interact with NFAT2 and NFAT4, we determined by DNA-binding activity ELISA which isoforms (i.e., Sp1 and Sp3) are activated by phenylephrine. In small immortalized cholangiocytes, phenylephrine stimulated Sp1 (but not Sp3), which was blocked by BAPTA/AM, CAI, and MiA (Fig. 7B,C).

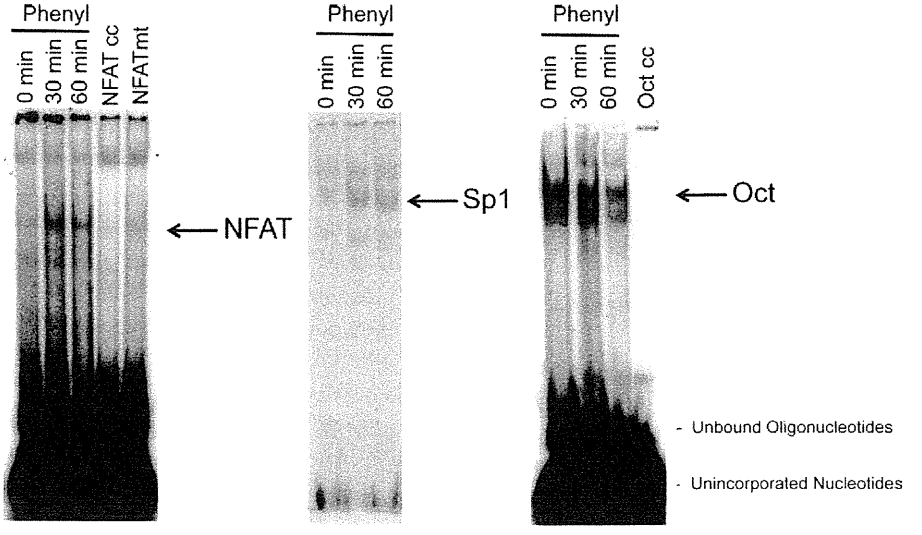

Fig. 6. Evaluation of phenylephrine-induced NFAT and Sp1 DNA-binding activity by EMSA. Immortalized small cholangiocytes were stimulated with phenylephrine for 0, 30, and 60 minutes at 37°C and DNA-binding activity was assessed by EMSA. Phenylephrine stimulated a time-dependent increase in DNA-binding for both NFAT (NFAT2 and 4 can both bind the consensus sequence) and Sp1. DNA-binding activity to the Oct consensus sequence was used as a loading control. Specificity of binding was demonstrated by adding 50-fold excess of either unlabeled NFAT consensus sequence, (NFAT cc), mutated NFAT consensus sequence (NFAT mt), or Oct sequence to the nuclear extract taken at time 0. NFAT = nuclear factor of activated T cells; NFAT cc = NFAT cold consensus sequence; NFAT mt = NFAT mutated competitor; Oct = octamer binding factor; and Oct cc = Oct cold consensus sequence.

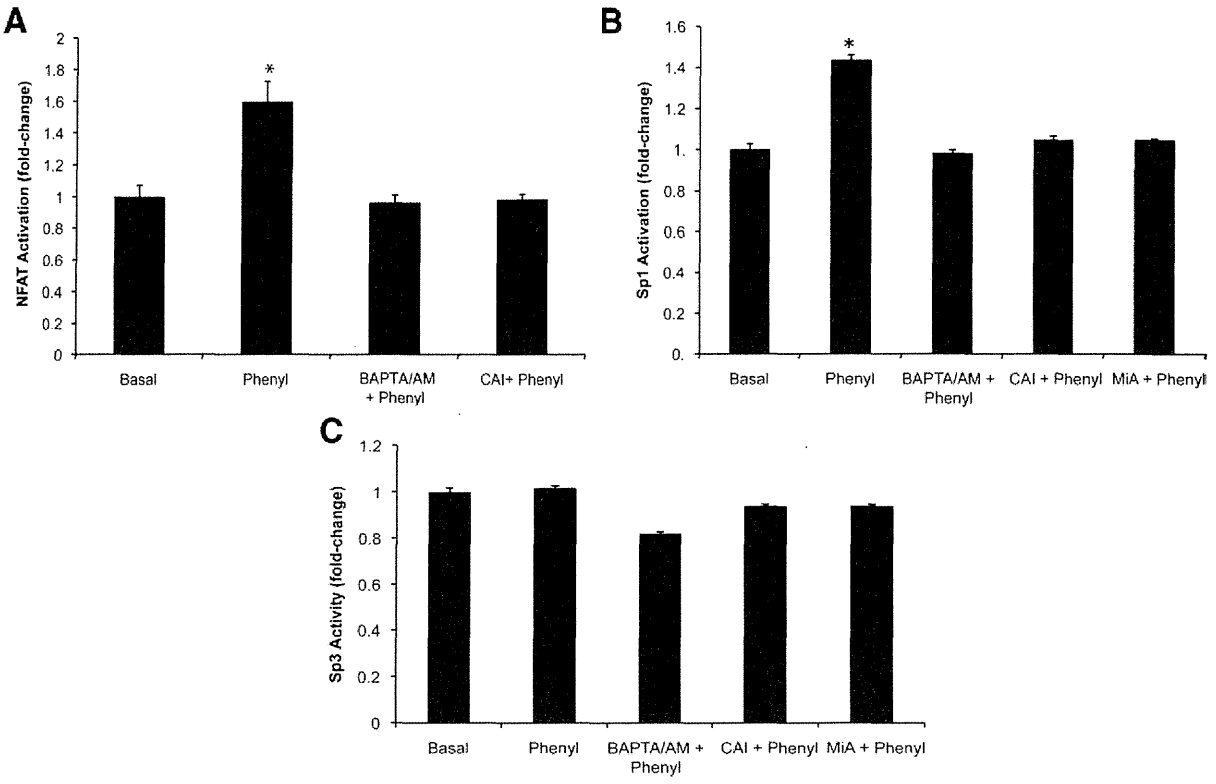

Fig. 7. Phenylephrine induces NFAT2 and Sp1 (but not Sp3) DNA-binding activity. (A) Immortalized small cholangiocytes were stimulated with phenylephrine in the presence/absence of BAPTA/AM and CAI for 60 minutes. NFAT2 DNA-binding activity was determined by ELISA. Phenylephrine stimulates the DNA-binding activity of NFAT2, which is blocked by BAPTA/AM and CAI. Asterisk (*) denotes significance ($P < 0.05$) when compared with the respective basal treatment using a t test ($n = 4$). (B,C) Small cholangiocytes were stimulated with phenylephrine in the presence/absence of BAPTA/AM, CAI and MiA for 60 minutes. Sp1 and Sp3 DNA-binding activity was determined by ELISA. Phenylephrine stimulates the DNA-binding activity of Sp1 (B), but not Sp3 (C), which is blocked by BAPTA/AM, CAI, and MiA. Asterisk (*) denotes significance ($P < 0.05$) when compared with the respective basal treatment using a t test ($n = 4$).

Knockdown of NFAT2 and Sp1 Expression in Immortalized Small Cholangiocytes Prevents Phenylephrine-Induced Proliferation. We established small cholangiocyte lines that have NFAT2, NFAT4, and Sp1 expression stably knockdown. Knockdown of NFAT2 expression prevented phenylephrine stimulated proliferation of small cholangiocytes (Fig. 8A). Knockdown of NFAT4 only slightly depressed phenylephrine-stimulated proliferation of small cholangiocytes (Fig. 8B). In NFAT4 knockdown cells, phenylephrine stimulated a significant increase in small cholangiocyte proliferation versus basal (Fig. 8B). Phenylephrine had no effect on small cholangiocyte proliferation in cells with knockdown of Sp1 expression (Fig. 8B).

Discussion

We demonstrated that: (1) small and large bile ducts and freshly isolated and immortalized cholangiocytes express all of the AR subtypes; (2) NFAT2 and NFAT4 are predominantly expressed by small bile ducts and immortalized small cholangiocytes; (3) phenylephrine stimulates both *in vivo* and *in vitro* the proliferation of small cholangiocytes via activation of Ca^{2+}-dependent signaling, which is blocked by *in vivo* and *in vitro* inhibition of NFAT and Sp1; (4) phenylephrine stimulates Ca^{2+}-dependent DNA-binding activities of NFAT2 and Sp1 (but not Sp3) and nuclear translocation of NFAT2 and NFAT4 in immortalized small cholangiocytes; and (5) knockdown of NFAT2 or Sp1 gene expression prevents phenylephrine-induced small cholangiocyte proliferation, whereas NFAT4 knockdown had a minimal effect on phenylephrine-induced proliferation of immortalized small cholangiocytes. The regulation of small cholangiocyte proliferation (via activation of α_{1A}, α_{1B}, α_{1D} AR by phenylephrine) is dependent on activation of Ca^{2+}/NFAT2/Sp1 signaling mechanisms.

The possible influence on the results by using small and large immortalized cholangiocytes are minimal, because these cells are derived from small and large

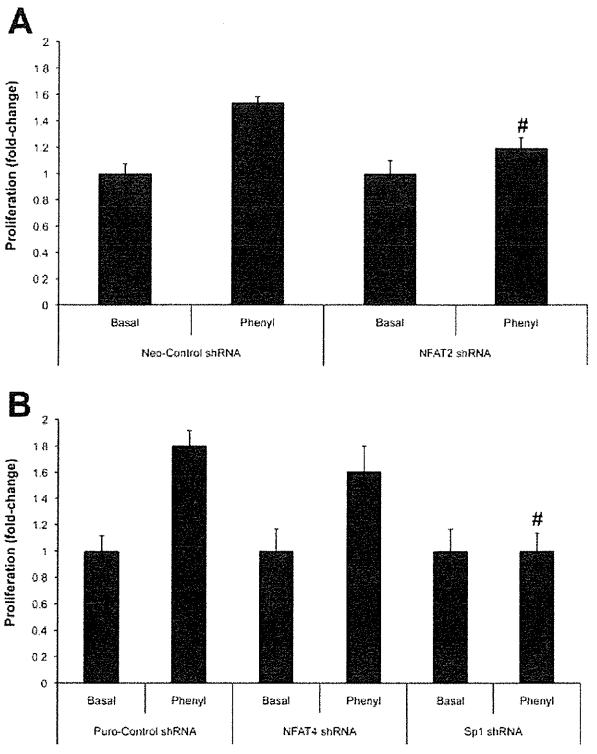

Fig. 8. Knockdown of NFAT2 and Sp1 expression prevents phenylephrine-induced proliferation of immortalized small cholangiocytes. The expression of NFAT2, NFAT4, or Sp1 was knockdown in small cholangiocytes by stable transfection of the respective shRNA. The knockdown of NFAT2 (A) and Sp1 (B) resulted in the prevention of phenylephrine-stimulated small cholangiocyte proliferation. (B) Knockdown of the expression NFAT4 did not significantly inhibit phenylephrine stimulation of small cholangiocyte proliferation. Data was expressed as fold-change relative to the respective basal values. Hash mark (£) denotes significance ($P < 0.05$) when compared with the respective phenyl-stimulated treatment group using a t test (n = 7).

bile ducts[5,6]; and have similar morphological, phenotypical and functional characteristics of freshly isolated small and large murine cholangiocytes.[5,6,35] These cell preparations express similar levels of the biliary markers, cytokeratin-7 and cytokeratin-19,[5,6] and display similar morphological differences in size.[5,6] At the functional level immortalized large (but not small) cholangiocytes express secretin receptor, CFTR and Cl^-/HCO_3-exchanger and selectively respond to secretin with changes in cAMP levels similar to that of freshly isolated cholangiocytes.[5,6] Immortalized small and large cholangiocytes display proliferative capacities similar to freshly isolated small and large mouse cholangiocytes because large cholangiocytes proliferate by a cAMP-dependent pathway, whereas IP_3/Ca^{2+}-dependent signalings regulate the growth of small cholangiocytes.[5,6,15] These findings support the validity of immortalized small and large cholangiocytes for evaluating functions of small and large bile ducts.

Small and large cholangiocytes express α_1-AR (α_{1A}, α_{1B}, α_{1D}). However, only immortalized small cholangiocytes respond *in vitro* to phenylephrine with increased proliferation that was blocked by all three α_1-AR antagonists (Fig. 4C). Although dobutamine induced *in vitro* a significant increase in the proliferation of immortalized small cholangiocytes, we did not address the mechanisms of such increase because dobutamine is a racemic mixture, in which one enantiomer is an agonist at $\beta 1$ and $\beta 2$ AR, and the other enantiomer is an agonist at α_1 AR.[36] Thus, dobutamine-induced increases in small cholangiocyte proliferation may be due to the activation of α_1 AR. A specific $\beta 1$-AR agonist is not available. We have demonstrated that phenylephrine increases secretin-induced choleresis of large cholangiocytes when administered to bile duct–ligated rats.[10] In *in vitro* studies, phenylephrine did not alter basal but increased secretin-stimulated large bile duct secretory activity and cAMP levels, which were blocked by BAPTA/AM and Gö6976 (a PKC antagonist).[10] Phenylephrine increased IP_3 and Ca^{2+} levels and activated PKCα and PKCβ_{II}.[10] Because large cholangiocytes are normally hormonally responsive to secretin[16,37] and regulated by cAMP-dependent signaling,[3,16,23] we propose that this acute effect of phenylephrine on secretin-stimulated large bile duct secretion is likely mediated by activation of the Ca^{2+}-dependent adenylyl cyclase, AC8, which is key in the secretory activity of large cholangiocytes.[38] We postulated that phenylephrine has differential effects on small and large cholangiocytes. In immortalized small cholangiocytes, phenylephrine stimulated intracellular IP_3 levels and plays a role in stimulating proliferation. Activation of small cholangiocyte proliferation by endogenous catecholamines (such as, norepinephrine and epinephrine) and other Ca^{2+} agonists (including phenylephrine) may be key during pathological conditions when large cholangiocytes are damaged, and the *de novo* proliferation of small cholangiocytes is necessary for the replenishment of the biliary system and compensation for loss of hormonal responsiveness.[3,7] Other studies have shown that α_1-AR agonists like phenylephrine can induce proliferation in various cell types including hepatocytes.[39] We found a similar profile in small cholangiocytes, because phenylephrine-induced proliferation was blocked by inhibition of Ca^{2+}, calcineurin activity, and NFAT activity. In addition, phenylephrine-induced proliferation was blocked by MiA implicating the involvement of Sp1/3.

NFAT and Sp1/3 isoforms play a critical role in the regulation of cell proliferation. NFAT2 stimulates proliferation of several cell types including lymphocytes.[40] NFAT4 deficiency results in incomplete liver regeneration following partial hepatectomy.[41] NFAT2 and 4 have also been shown to crosstalk with Sp1/Sp3 to cooperatively regulate membrane type 1 matrix metalloproteinase gene transcription and cellular differentiation in keratinocytes.[42] Using several molecular approaches, we found that phenylephrine stimulates the Ca^{2+}-dependent DNA-binding activities of NFAT2/4, and Sp1 (but not Sp3) and the nuclear translocation of NFAT2 and NFAT4 suggesting the involvement of these transcription factors in phenylephrine-induced proliferation of small cholangiocytes. We confirmed their involvement using shRNA to knockdown the expression of these transcription factors.

In summary, we demonstrated that small cholangiocyte proliferation is regulated by the activation of α_1-ARs and occurs through Ca^{2+}/calcineurin-dependent activation of NFAT2 and Sp1. Modulation of the Ca^{2+}-dependent transcription factors, NFAT2 and SP1, may be an important therapeutic approach for inducing ductular proliferation for maintaining the homeostasis of the biliary during the damage of large cAMP-responsive bile ducts.[1,3,7]

Acknowledgment: We thank Anna Webb of the Texas A&M Health Science Center Microscopy Imaging Center for assistance with confocal microscopy and Bryan Moss (Medical Illustration, Scott & White) for the help on the preparation of the figures and Dr. Marco Marzioni (Università Politecnica delle Marche, Italy) for the comments related to the revision of the manuscript.

References

1. Alpini G, Prall RT, LaRusso NF. The pathobiology of biliary epithelia. In: Arias IM, Boyer JL, Chisari FV, Fausto N, Jakoby W, Schachter D, et al. eds. The Liver: Biology and Pathobiology, 4th ed. Philadelphia, PA: Lippincott Williams & Wilkins; 2001:421-435.
2. Alpini G, Glaser S, Ueno Y, Pham L, Podila PV, Caligiuri A, et al. Heterogeneity of the proliferative capacity of rat cholangiocytes after bile duct ligation. Am J Physiol Gastrointest Liver Physiol 1998;274: G767-G775.
3. LeSage G, Glaser S, Marucci L, Benedetti A, Phinizy JL, Rodgers R, et al. Acute carbon tetrachloride feeding induces damage of large but not small cholangiocytes from BDL rat liver. Am J Physiol Gastrointest Liver Physiol 1999;276:G1289-G1301.
4. Francis H, Glaser S, Ueno Y, LeSage G, Marucci L, Benedetti A, et al. cAMP stimulates the secretory and proliferative capacity of the rat intrahepatic biliary epithelium through changes in the PKA/Src/MEK/ERK1/2 pathway. J Hepatol 2004;41:528-537.
5. Ueno Y, Alpini G, Yahagi K, Kanno N, Moritoki Y, Fukushima K, et al. Evaluation of differential gene expression by microarray analysis in small and large cholangiocytes isolated from normal mice. Liver Int 2003;23:449-459.
6. Francis H, Glaser S, DeMorrow S, Gaudio E, Ueno Y, Venter J, et al. Small mouse cholangiocytes proliferate in response to H1 histamine receptor stimulation by activation of the IP3/CAMK I/CREB pathway. Am J Physiol Cell Physiol 2008;295:C499-C513.
7. Mancinelli R, Franchitto A, Gaudio E, Onori P, Glaser S, Francis H, et al. After damage of large bile ducts by gamma-aminobutyric acid, small ducts replenish the biliary tree by amplification of calcium-dependent signaling and de novo acquisition of large cholangiocyte phenotypes. Am J Pathol Gastrointest Liver Physiol 2010;176:1790-1800.
8. Francis H, LeSage G, DeMorrow S, Alvaro D, Ueno Y, Venter J, et al. The alpha2-adrenergic receptor agonist UK 14,304 inhibits secretin-stimulated ductal secretion by downregulation of the cAMP system in bile duct-ligated rats. Am J Physiol Cell Physiol 2007;293:C1252-C1262.
9. Glaser S, Alvaro D, Francis H, Ueno Y, Marucci L, Benedetti A, et al. Adrenergic receptor agonists prevent bile duct injury induced by adrenergic denervation by increased cAMP levels and activation of Akt. Am J Physiol Gastrointest Liver Physiol 2006;290:G813-G826.
10. LeSage G, Alvaro D, Glaser S, Francis H, Marucci L, Roskams T, et al. Alpha-1 adrenergic receptor agonists modulate ductal secretion of BDL rats via Ca(2+)- and PKC-dependent stimulation of cAMP. HEPATOLOGY 2004;40:1116-1127.
11. Hein P, Michel MC. Signal transduction and regulation: are all alpha1-adrenergic receptor subtypes created equal? Biochem Pharmacol 2007; 73:1097-1106.
12. Nguyen T, Di Giovanni S. NFAT signaling in neural development and axon growth. Int J Dev Neurosci 2008;26:141-145.
13. Lipskaia L, Lompre AM. Alteration in temporal kinetics of Ca2+ signaling and control of growth and proliferation. Biol Cell 2004;96: 55-68.
14. Ho SN. The role of NFAT5/TonEBP in establishing an optimal intracellular environment. Arch Biochem Biophys 2003;413:151-157.
15. Glaser S, Gaudio E, Rao A, Pierce LM, Onori P, Franchitto A, et al. Morphological and functional heterogeneity of the mouse intrahepatic biliary epithelium. Lab Invest 2009;89:456-469.
16. Alpini G, Roberts S, Kuntz SM, Ueno Y, Gubba S, Podila PV, et al. Morphological, molecular, and functional heterogeneity of cholangiocytes from normal rat liver. Gastroenterology 1996;110:1636-1643.
17. Alpini G, Ulrich C, Roberts S, Phillips JO, Ueno Y, Podila PV, et al. Molecular and functional heterogeneity of cholangiocytes from rat liver after bile duct ligation. Am J Physiol Gastrointest Liver Physiol 1997; 272:G289-G297.
18. Marinese D, Patel R, Walden PD. Mechanistic investigation of the adrenergic induction of ventral prostate hyperplasia in mice. Prostate 2003;54:230-237.
19. Noguchi H, Matsushita M, Okitsu T, Moriwaki A, Tomizawa K, Kang S, et al. A new cell-permeable peptide allows successful allogeneic islet transplantation in mice. Nat Med 2004;10:305-309.
20. Jia Z, Gao Y, Wang L, Li Q, Zhang J, Le X, et al. Combined treatment of pancreatic cancer with mithramycin A and tolfenamic acid promotes Sp1 degradation and synergistic antitumor activity. Cancer Res 2010;70:1111-1119.
21. LeSage G, Glaser S, Gubba S, Robertson WE, Phinizy JL, Lasater J, et al. Regrowth of the rat biliary tree after 70% partial hepatectomy is coupled to increased secretin-induced ductal secretion. Gastroenterology 1996;111:1633-1644.
22. Onori P, Wise C, Gaudio E, Franchitto A, Francis H, Carpino G, et al. Secretin inhibits cholangiocarcinoma growth via dysregulation of the cAMP-dependent signaling mechanisms of secretin receptor. Int J Cancer 2010;127:43-54.
23. Francis H, Franchitto A, Ueno Y, Glaser S, DeMorrow S, Venter J, et al. H3 histamine receptor agonist inhibits biliary growth of BDL rats by downregulation of the cAMP-dependent PKA/ERK1/2/ELK-1 pathway. Lab Invest 2007;87:473-487.
24. Oriowo MA, Chapman H, Kirkham DM, Sennitt MV, Ruffolo RR Jr, Cawthorne MA. The selectivity in vitro of the stereoisomers of the beta-3 adrenoceptor agonist BRL 37344. J Pharmacol Exp Ther 1996; 277:22-27.

25. Jia Z, Zhang J, Wei D, Wang L, Yuan P, Le X, et al. Molecular basis of the synergistic antiangiogenic activity of bevacizumab and mithramycin A. Cancer Res 2007;67:4878-4885.
26. Ford AP, Arredondo NF, Blue DR Jr, Bonhaus DW, Jasper J, Kava MS, et al. RS-17053 (N-[2-(2-cyclopropylmethoxyphenoxy)ethyl]-5-chloro-alpha, alpha-dimethyl-1H-indole-3-ethanamine hydrochloride), a selective alpha 1A-adrenoceptor antagonist, displays low affinity for functional alpha 1-adrenoceptors in human prostate: implications for adrenoceptor classification. Mol Pharmacol 1996;49:209-215.
27. Morton JS, Daly CJ, Jackson VM, McGrath JC. α1A-Adrenoceptors mediate contractions to phenylephrine in rabbit penile arteries. Br J Pharmacol 2007;150:112-120.
28. Goetz AS, King HK, Ward SD, True TA, Rimele TJ, Saussy DLJ. BMY is 7378 is a selective antagonist of the D subtype of alpha 1-adrenoceptors. Eur J Pharmacol 1995;272:R5-R6.
29. Ma P, Wang Z, Pflugfelder SC, Li DQ. Toll-like receptors mediate induction of peptidoglycan recognition proteins in human corneal epithelial cells. Exp Eye Res 2010;90:130-136.
30. Goodenough S, Davidson M, Chen W, Beckmann A, Pujic Z, Otsuki M, et al. Immediate early gene expression and delayed cell death in limbic areas of the rat brain after kainic acid treatment and recovery in the cold. Exp Neurol 1997;145:451-461.
31. Fuchs R, Stelzer I, Haas HS, Leitinger G, Schauenstein K, Sadjak A. The alpha1-adrenergic receptor antagonists, benoxathian and prazosin, induce apoptosis and a switch towards megakaryocytic differentiation in human erythroleukemia cells. Ann Hematol 2009;88:989-997.
32. Badran BM, Wolinsky SM, Burny A, Willard-Gallo KE. Identification of three NFAT binding motifs in the 5′-upstream region of the human CD3gamma gene that differentially bind NFATc1, NFATc2, and NF-kappa B p50. J Biol Chem 2002;277:47136-47148.
33. DeMorrow S, Francis H, Gaudio E, Ueno Y, Venter J, Onori P, et al. Anandamide inhibits cholangiocyte hyperplastic proliferation via activation of thioredoxin 1/redox factor 1 and AP-1 activation. Am J Physiol Gastrointest Liver Physiol 2008;294:G506-G519.
34. O-Uchi J, Komukai K, Kusakari Y, Obata T, Hongo K, Sasaki H, et al. alpha1-adrenoceptor stimulation potentiates L-type Ca2+ current through Ca2+/calmodulin-dependent PK II (CaMKII) activation in rat ventricular myocytes. Proc Natl Acad Sci U S A 2005;102:9400-9405.
35. Glaser S, Lam IP, Franchitto A, Gaudio E, Onori P, Chow BK, et al. Knockout of secretin receptor reduces large cholangiocyte hyperplasia in mice with extrahepatic cholestasis induced by bile duct ligation. HEPATOLOGY 2010;52:204-214.
36. Brunton L, Blumenthal D, Buxton I, Parker K. Goodman & Gilman's Manual of Pharmacology and Therapeutics. New York: McGraw-Hill Medical; 2008:159.
37. Alpini G, Glaser S, Robertson W, Rodgers RE, Phinizy JL, Lasater J, et al. Large but not small intrahepatic bile ducts are involved in secretin-regulated ductal bile secretion. Am J Physiol Gastrointest Liver Physiol 1997;272:G1064-G1074.
38. Strazzabosco M, Fiorotto R, Melero S, Glaser S, Francis H, Spirli C, et al. Differentially expressed adenylyl cyclase isoforms mediate secretory functions in cholangiocyte subpopulation. HEPATOLOGY 2009;50:244-252.
39. Han C, Bowen WC, Michalopoulos GK, Wu T. Alpha-1 adrenergic receptor transactivates signal transducer and activator of transcription-3 (Stat3) through activation of Src and epidermal growth factor receptor (EGFR) in hepatocytes. J Cell Physiol 2008;216:486-497.
40. Yoshida H, Nishina H, Takimoto H, Marengere LE, Wakeham AC, Bouchard D, et al. The transcription factor NF-ATc1 regulates lymphocyte proliferation and Th2 cytokine production. Immunity 1998;8:115-124.
41. Pierre KB, Jones CM, Pierce JM, Nicoud IB, Earl TM, Chari RS. NFAT4 deficiency results in incomplete liver regeneration following partial hepatectomy. J Surg Res 2009;154:226-233.
42. Santini MP, Talora C, Seki T, Bolgan L, Dotto GP. Cross talk among calcineurin, Sp1/Sp3, and NFAT in control of p21(WAF1/CIP1) expression in keratinocyte differentiation. Proc Natl Acad Sci U S A 2001;98:9575-9580.

ウイルス感染とPBC

二宮匡史* 福島耕治*
上野義之* 下瀬川徹*

索引用語：NOD.c3c4マウス，レトロウイルス，原発性胆汁性肝硬変，Mouse mammary tumor virus

1 はじめに

原発性胆汁性肝硬変(PBC)は，1851年にAddisonらにより報告された，肝内胆管の進行性破壊と消失が特徴的な原因不明の疾患である[1]．病理組織学的には，慢性非化膿性破壊性胆管炎と肉芽腫形成を特徴とし，胆管上皮細胞の変性・壊死が生じ，慢性的に胆汁うっ滞が起こる．PBCは自己抗体の抗ミトコンドリア抗体(AMA)の出現が特徴的であり，ミトコンドリア内膜に存在する抗原を認識する[2,3]．抗原として，4つのM2蛋白が存在しており，それらはミトコンドリア酵素であるピルビン酸デヒドロゲナーゼ複合体(PDC)の成分である[4]．その中でも，PDC-E2は種を超えて保存されており，AMAが大腸菌由来のPDC-E2と交差反応を示すことから，胆管細胞障害には，細胞障害性T細胞が重要な役割を担い，病態発生の要因として大腸菌関与が推測されている[5,6]．他にも，組織学的な見地から，胆管周囲の浸潤細胞はT細胞優位であり，小葉間胆管上皮細胞表面にはHLAクラスII抗原の異所性発現がみられ，クラスI抗原の発現の増強も認められる．胆管上皮細胞に対して，アポトーシスの選択的誘導や，Xenobioticへの暴露による抗原の変化なども報告されている[7]．

その中で以前より，PBCの発症原因として，ウイルスもしくは，ウイルス関連因子の関与も推察されている．この根拠として，PBCは血清IgM値の高値が特徴的であり，IgMは抗原特異的なIgG反応の増強に関わり，自然免疫において，感染微生物に対する最初の防御機構をつかさどっている．また，PBC患者では血中IgG3濃度が高く，末梢血リンパ球からの分泌が亢進していることが報告されている[8,9]．IgG3は各種ウイルス感染の初感染で産生される．

本稿では，PBCの病因としてのウイルス感染に関するこれまでの報告をまとめ，PBCの動物モデルとされるNOD.c3c4マウスの解析結果と合わせ，ウイルス感染症との関連性

Masashi NINOMIYA et al: Viral infection associated with PBC
*東北大学大学院医学系研究科消化器病態学［〒980-8574 宮城県仙台市青葉区星陵町1-1］

について紹介する．

2 PBCとウイルス感染の報告

1．レトロウイルス

1988年にMunozらが，human immunodeficiency virus-1（HIV-1）に対する抗体がPBC患者血清中に存在していることを報告した[10]．HIV-1が産生するp24gag蛋白に対する抗体を調べたところシェーグレン症候群で30％，健常者では1％未満の検出率で[11]，全身性エリテマトーデス（SLE）では36％，同様の抗体が検出され，自己免疫疾患のHIV-1の関与が示唆された[12]．Masonらも，p24gag蛋白に対する抗体を調べた結果，PBCで35％，SLEで29％，原発性硬化性胆管炎（PSC）で39％検出されたが，アルコール性肝障害，健常者ではそれぞれ4％の検出率であった．さらに，human intracisternal A-type particle（HIAP）に対する抗体を調べ，PBCの51％で認められたが，アルコール性肝障害では認めず，健常者では4％検出された．これらレトロウイルスが産生する蛋白に対する抗体を調べた結果，PBCを含めた自己免疫性疾患で有意に検出され，レトロウイルスの蛋白に対する免疫反応が病態に関与していることが示唆された[13]．

2003年にXuらは，胆管上皮細胞のcDNAライブラリーから，mouse mammary tumor virus（MMTV）とヒトの乳癌組織から同定されたレトロウイルスの部分的なポリメラーゼ領域の塩基配列と類似したDNA fragmentを検出した[14,15]．また，PBCの肝組織からはみいだせなかったが，末梢リンパ節よりMMTVの蛋白を検出している．PBC患者へのラミブジン単独投与とラミブジン＋ジドブジン投与のパイロット研究にて，単独投与群では，組織，血清学的な改善は認めなかったが，併用療法群では，有意な組織学的改善が認められ，一部で血清学的な改善も報告されている[16]．その後，PBC患者に対してラミブジン＋ジドブジン投与群vsプラサボ投与群に分けてRandomized試験が行われている．抗ウイルス薬投与群において血清学上，クリニカルスコアの改善とウイルス消失の割合に有意な差が認められた[17]．ただ，同時期にSelmiらは，PBC患者の血清，肝組織，末梢リンパ節からMMTV関連分子や蛋白に対する抗体は認められないと報告しており，現時点ではMMTV感染とPBC発症の関連性は結論に達していない[18]．われわれのRCTでも逆転写酵素阻害剤であるラミブジンをUDCA不応性のPBC患者に投与する試験でもその効果は明らかでなかった．しかし，ウイルスの関与自体が明らかでなく，必然的に応答を評価すべくアッセイ系も存在しないため，その評価はいまだ不明である[19]．

2．その他のウイルス

1992年にMorshedらは，PBC患者の末梢血単核球，肝組織，唾液からEpstein Barr virus（EBV）-DNAをPCR法にて他肝疾患患者や健常者と比較し，高率に検出したと報告し，PBC患者はEBVに対して免疫反応が低下し，病態形成に関与している可能性を報告した[20]．さらに，2007年にBarzilaiらはコントロール群に比べ，PBC患者の血清からEBV early antigen IgGの抗体値が高いことを報告している[21]．また，Cytomegalovirus IgMの抗体価が高値であることも示している[21]．

3 NOD.c3c4マウスの解析とウイルス感染

2006年，IrieらによりNOD.c3c4マウスがPBCの動物モデルとして報告された．この

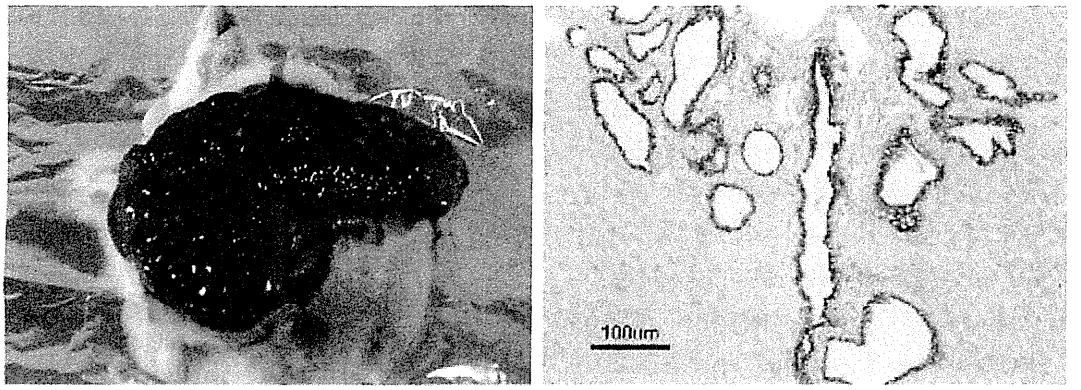

図1　胆管嚢胞を形成したNOD.c3c4マウスの肉眼像と組織像(ケラチン染色)

マウスは組織学的には，胆管周囲にT細胞を中心とした浸潤を認め，胆管の破壊，肉芽腫の形成，さらに血清学的にPDC-E2に対する抗体産生を生じるといったヒトのPBCに特徴的な要素を持っている[22]．しかし，相違点として，ヒトのPBCは胆管の破壊や消失を認めるが，このマウスでは多数の胆管嚢胞を形成する[23]．われわれはこのマウスの胆管細胞の遺伝子発現をMicroarrayにて解析したところ，Fas antigenの発現の低下を認めた[24]．ヒトのPBCの胆管細胞ではFas anitigenの増強が報告されており，CD4陽性リンパ球がFas/Fas ligandを介して直接的に細胞障害に関わることや，細胞障害性Tリンパ球がこのligandを介してApoptosisの誘導し，胆管細胞の消失に関与していることが推測される[25~27]．しかし，NOD.c3c4マウスではそのような機能が低下し，胆管細胞のApoptosisが起こりにくいため，このような嚢胞形成が生じると考えられた(図1)[24]．しかし，遺伝子発現に差がないにも関わらず，個体によって嚢胞形成の程度に差があるため，他の要因もあることが考えられた．

2007年にChenらは，リアルタイムPCRを用いてMMTVのgagとpol領域の類似の塩基配列がNOD.c3c4マウスの肝組織内に存在すること，免疫染色にてMMTVのカプシド蛋白が胆管の嚢胞部位に認められことを報告した[28]．さらに，NOD.c3c4マウスに対してラミブジン＋ジドブジン投与を試みたところ，コントロール群に比べ，胆管周囲の炎症の改善と，MMTVのウイルス量の低下を報告している．ただ，嚢胞形成に関しては明らかな差はなかった[29]．他にも，Grahamらは，NOD.c3c4マウスに逆転写酵素阻害薬にプロテアーゼ阻害薬を加えたプロトコールで投与を行い，胆管炎所見が完全に改善することを報告している[30]．これらの結果から，PBCの動物モデルであるNOD.c3c4マウスの病態形成にウイルス感染または，ウイルス関連因子が関与していることが示唆されている．

4　今後の展望

現時点ではPBCの病態発生機序は，AMAが大腸菌などの微生物由来のPDC-E2もしくはこの類似のモチーフに対して，交差反応性を示すことから，微生物由来ペプチドとの分子相同性による自己免疫反応を起こすことが，有力な仮説であろう．本稿では，過去のPBCとウイルス感染の既報とPBCモデルマウスのウイルス感染の可能性についてまとめたが，PBCの病態発生機序を解明するには

全く至っていない.

ウイルスの病原性の機序を証明するためには，ウイルスゲノムの複製や転写などの増殖機構，指向性といったウイルス側因子とともに，宿主細胞内でのさまざまなシグナル伝達系の変化，インテグレートされた状態，そしてそれらが免疫系とどのように反応するか，さらにその破綻の鍵となる瞬間などを理解し，解明していくことが必要である．そのため，現在の報告だけでは，PBCの病態発生の原因をウイルス感染と関連づけるのは，尚早であろう．他にもPBCだけでなく，AIH，PSCも病態発症に微生物の関与の可能性が考えられる．現代ではこれまでにない速度でバイオテクノロジーは進歩しており，自己免疫性の肝疾患についてもより精度が高い最新の技術を用いた新規の切り口が当然与えられる．これからのこれらの技術を応用した研究，報告が待たれるところである．

文　献

1) Addsion T, Gull W : On a certain affection of the skin vitiligoidea-α plana, β tuberosa. Guy's Hosp Rep 265–276, 1851
2) Nakanuma Y, Ohta G : Histometric and serial section observations of the intrahepatic bile ducts in primary biliary cirrhosis. Gastroenterology 76 : 1326–1332, 1979
3) Kaplan MM : Primary biliary cirrhosis. N Engl J Med 335 : 1570–1580, 1996
4) Gershwin M, Mackay I, Sturgess A : Identification and specificity of a cDNA encoding the 70 kd mitochondrial antigen recognized in primary biliary cirrhosis. J Immunol 138 : 3525–3531, 1987
5) Fussey SP, Ali ST, Guest JR et al : Reactivity of primary biliary cirrhosis sera with Escherichia coli dihydrolipoamide acetyltransferase (E2p) : characterization of the main immunogenic region. Proc Natl Acad Sci USA 87 : 3987–3991, 1990
6) Surh CD, Ahmed-Ansari A, Gershwin ME : Comparative epitope mapping of murine monoclonal and human autoantibodies to human PDH-E2, the major mitochondrial autoantigen of primary biliary cirrhosis. J Immunol 144 : 2647–2652, 1990
7) Selmi C, Gershwin ME : The etiology mystery in primary biliary cirrhosis. Dig Dis 28 : 105–115, 2010
8) Bird P, Calvert JE, Mitchison H et al : Lymphocytes from patients with primary biliary cirrhosis spontaneously secrete high levels of IgG3 in culture. Clin Exp Immunol 71 : 475–480, 1988
9) Surh CD, Cooper AE, Coppel RL et al : The predominance of IgG3 and IgM isotype antimitochondrial autoantibodies against recombinant fused mitochondrial polypeptide in patients with primary biliary cirrhosis. Hepatology 8 : 290–295, 1988
10) Munoz S, Ballas S, Norberg R et al : Antibodies to human immunodeficiency virus (HIV) in primary biliary cirrhosis. Gastroenterology 94 : A574, 1988
11) Talal N, Dauphinee MJ, Dang H et al : Detection of serum antibodies to retroviral proteins in patients with primary Sjogren's syndrome (autoimmune exocrinopathy) . Arthritis Rheum 33 : 774–781, 1990
12) Talal N, Garry RF, Schur PH et al : A conserved idiotype and antibodies to retroviral proteins in systemic lupus erythematosus. J Clin Invest 85 : 1866–1871, 1990
13) Mason AL, Xu L, Guo L et al : Detection of retroviral antibodies in primary biliary cirrhosis and other idiopathic biliary disorders. Lancet 351 : 1620–1624, 1998
14) Xu L, Shen Z, Guo L et al : Does a betaretrovirus infection trigger primary biliary cirrhosis? Proc Natl Acad Sci USA 100 : 8454–8459, 2003
15) Xu L, Sakalian M, Shen Z et al : Cloning the human betaretrovirus proviral genome from patients with primary biliary cirrhosis. Hepatology 39 : 151–156, 2004
16) Mason AL, Farr GH, Xu L et al : Pilot studies of single and combination antiretroviral therapy in patients with primary biliary cirrhosis. Am J Gastroenterol 99 : 2348–2355, 2004
17) Mason AL, Lindor KD, Bacon BR et al : Clinical Trial: Randomized controlled trial of zidovudine and lamivudine for patients with primary

biliary cirrhosis stabilized on ursodiol. Aliment Pharmacol Ther 2008
18) Selmi C, Ross SR, Ansari AA et al : Lack of immunological or molecular evidence for a role of mouse mammary tumor retrovirus in primary biliary cirrhosis. Gastroenterology 127 : 493–501, 2004
19) Fukushima K, Ueno Y, Shimosegawa T : Treatment of Primary Biliary Cirrhosis: A new challenge? Hepatol Res 40 : 61–68, 2010
20) Morshed SA, Nishioka M, Saito I et al : Increased expression of Epstein-Barr virus in primary biliary cirrhosis patients. Gastroenterol Jpn 27 : 751–758, 1992
21) Barzilai O, Sherer Y, Ram M et al : Epstein-Barr virus and cytomegalovirus in autoimmune diseases: are they truly notorious? A preliminary report. Ann N Y Acad Sci 1108 : 567–577, 2007
22) Irie J, Wu Y, Wicker LS et al : NOD.c3c4 congenic mice develop autoimmune biliary disease that serologically and pathogenetically models human primary biliary cirrhosis. J Exp Med 203 : 1209–1219, 2006
23) Locke GR 3rd, Therneau TM, Ludwig J et al : Time course of histological progression in primary biliary cirrhosis. Hepatology 23 : 52–56, 1996
24) Nakagome Y, Ueno Y, Kogure T et al : Autoimmune cholangitis in NOD.c3c4 mice is associated with cholangiocyte-specific Fas antigen deficiency. J Autoimmun 29 : 20–29, 2007
25) Nagata S, Golstein P : The Fas death factor. Science 267 : 1449–1456, 1995
26) Ueno Y, Ishii M, Yahagi K et al : Fas-mediated cholangiopathy in the murine model of graft versus host disease. Hepatology 31 : 966–974, 2000
27) Iwata M, Harada K, Hiramatsu K et al : Fas ligand expressing mononuclear cells around intrahepatic bile ducts co-express CD68 in primary biliary cirrhosis. Liver 20 : 129–135, 2000
28) Chen M, Graham D, Zhang G et al : Biliary infection with mouse mammary tumor virus in the NOD.c3c4 mouse and other mouse models of primary biliary cirrhosis [Abstract]. Hepatology 46 : 551A, 2007
29) Chen M, Graham D, Girgis S et al : Combination antiretroviral therapy with Combivir attenuates autoimmune biliary disease in the NOD.c3c4 mouse model of primary biliary cirrhosis [Abstract]. Hepatology 46 : 548A, 2007
30) Graham D, Chen M, Girgis S et al : Highly active anti-retroviral therapy completely abrogates cholangitis in the NOD.c3c4 mouse model of PBC (Abstract) . Journal of Hepatology 2 : s54, 2008

*　　*　　*

Case Report

Serial Changes of Liver Stiffness Measured by Acoustic Radiation Force Impulse Imaging in Acute Liver Failure: A Case Report

Hidekatsu Kuroda, MD, Yasuhiro Takikawa, MD, Mio Onodera, MD, Keisuke Kakisaka, MD, Yuichi Yoshida, MD, Koujiro Kataoka, MD, Kei Sawara, MD, Yasuhiro Miyamoto, MD, Kanta Oikawa, MD, Ryujin Endo, MD, Kazuyuki Suzuki, MD

Division of Gastroenterology and Hepatology, Department of Internal Medicine, Iwate Medical University, School of Medicine, Uchimaru 19-1, Morioka, Iwate, 020-8505, Japan

Received 18 November 2010; accepted 19 September 2011

ABSTRACT: Acoustic radiation force impulse (ARFI) imaging is a new technology used to determine liver elasticity. We report the case of a patient that survived hyperacute-type acute liver failure (ALF) and who showed a dramatic change in the value of shear wave velocity (SWV) measured by ARFI, which corresponded with the severity of her liver damage. The value of SWV increased significantly up to 3.6 ± 0.3 m/s during the encephalopathy phase and then decreased along with the recovery of liver function, the blood flow of the right portal vein, and the liver volume. These findings suggest the value of SWV in ALF as a reliable marker of liver tissue damage. Further investigations of the pathophysiological significance of SWV in ALF are warranted. © 2011 Wiley Periodicals, Inc. *J Clin Ultrasound* **40**:99–104, 2012; Published online in Wiley Online Library (wileyonlinelibrary.com). DOI: 10.1002/jcu.20893

Keywords: acute liver failure; liver stiffness; ARFI; shear wave velocity; elastography

The severity of liver tissue damage and the prompt reconstruction of liver tissue in acute liver failure (ALF) are critical factors that impact the prognosis and determine the necessity for liver transplantation.[1,2] Although histopathological examination of biopsy specimens obtained through transvenous biopsy and various imaging methods such as CT can be used for this purpose, ALF patients are often too sick to undergo these examinations frequently and serially.[3,4] In contrast, sonography (US) can be performed on these patients at any time, because it is noninvasive and can be performed at the bedside.

Several previous reports using transient elastography (TE) have revealed that the degree of liver stiffness increased transiently during the acute phase of acute hepatitis.[5–7] Acoustic radiation force impulse (ARFI) imaging is a new reproducible technique for quantitative assessment of tissue stiffness through measurement of shear wave velocity (SWV),[8,9] and it has been applied to the evaluation of the extent of fibrosis in chronic liver disease.[10–12] However, no reports have assessed liver stiffness in ALF patients using ARFI.

We describe the case of a patient who recovered from hyperacute ALF without liver transplantation and underwent serial evaluations of liver stiffness using ARFI over the course of ALF and recovery.

CASE REPORT

A 52-year-old Japanese woman was evaluated because of general fatigue, jaundice, and upper abdominal pain for a few days. There was no history of drug or alcohol abuse or any family history of liver disease. Due to the development of disorientation, she was transferred to the liver unit of the Iwate Medical University Hospital. The initial laboratory examination showed severe liver dysfunction (Table 1). The serological tests

Correspondence to: H. Kuroda

TABLE 1
Laboratory Data on Admission

Hematology		Biochemistry			
WBC	15,400 /ul	T. Bil	4.0 mg/dl	BUN	21.7 mg/dl
RBC	449 × 10^4/ul	D/T ratio	0.80	CRNN	2.05 mg/dl
Hb	14.4 g/dl	AST	6,568 IU/l	Na	128 mEq/l
Ht	33.5 %	ALT	4,911 IU/l	K	5.4 mEq/l
Plt.	13.6 × 10^4/ul	LDH	1,511 IU/l	Cl	96 mEq/l
		γ-GTP	788 IU/l	TC	83 mg/dl
Coagulation		ChE	146 IU/l	BS	129 mg/dl
APTT	65.2 S	ALP	567 IU/l	CRP	0.4 mg/dl
PT (%)	5.0 %	AMY	320 IU/l	IgG	816 mg/dl
PT-INR	5.9	TP	4.4 g/dl	IgA	128 mg/dl
HPT	19.4 %	Alb	3.0 g/dl	IgM	40 mg/dl
		NH3	175 ug/dl		
Virus makers					
IgM-HA Ab	0.0	CMV IgM	<×10		
HBs Ag	0.1 C.O.I.	CMV IgG	<×10		
HBs Ab	0.1 C.O.I.	HSV IgM	<×10		
HBe Ag	0.1 C.O.I	HHV6 IgM	<×10		
HBe Ab	(−)	Parbo B19 IgM	(−)		
HBc Ab	(−)				
IgM-HBc Ab	0.2 C.O.I.	Serology			
HCV Ab	0.9 C.O.I.	ANA	(−)		
HCV RNA (PCR)	(−)	AMA	(−)		
HEV IgM	(−)	AM2A	(−)		
HEV IgG	(−)				
EBV VCA IgM	<×10	Others			
EBV VCA IgG	(+)	AFP	7.2 ng/ml		
EBV EBNA	(+)	hHGF	47.2 ng/ml		

Abbreviations, AFP, alpha-fetoprotein; Alb, aluminum; ALP, alkaline phosphatase; ALT, alanine transaminase; AMA, antimitochondrial antibody; AMY, amylase; ANA, antinuclear antibody; AM2A, antimitochondrial M2 antibody; APTT, activated partial thromboplastin time; AST, aspartate transaminase; BS, blood sugar; BUN, blood urea nitrogen; ChE, cholinesterase; Cl, chlorine; CMV IgG, cytomegalovirus immunoglobulin G; CMV IgM, cytomegalovirus immunoglobulin M; C.O.I., cutoff index; CRNN, creatinine; CRP, C-reactive protein; D/T ratio, direct bilirubin/total bilirubin ratio; EBV VCA EBV EBNA, Epstein-Barr virus nuclear antigen; EBV VCA IgG, Epstein-Barr virus antibody to viral capsid antigen, IgG; EBV VCA IgM, Epstein-Barr virus antibody to viral capsid antigen, IgM; γ-GTP, γ-glutamyltransferase; Hb, hemoglobin; HBc Ab, hepatitis B core antigen; HBe Ab, hepatitis B e antibody; HBs Ab, hepatitis B surface antibody; HBs Ag, hepatitis B surface antigen; HCVAb, hepatitis C virus antibody; HCV RNA, hepatitis C virus RNA; HEV IgG, immunoglobulin G antibodies against hepatitis E virus; HEV IgM, immunoglobulin M antibodies against hepatitis E virus; hHGF, human hepatocyte growth factor; HHV6 IgM, human herpes virus 6 immunoglobulin M; HSV IgM, herpes simplex virus immunoglobulin M; Ht, hematocrit; IgA, immunoglobulin A; IgG, immunoglobulin G; IgM, immunoglobulin M; IgM-HA Ab, immunoglobulin M antibody to hepatitis A; IgM-HBc Ab, immunoglobulin M antibody to hepatitis B core antigen; INR, international normalized ratio; K, potassium; LDH, lactate dehydrogenase; Na, natrium; NH3, ammonia; Parbo B19 IgM, parvovirus B19 immunoglobulin M; Plt., platelet counts; PT, prothrombin time; RBC, red blood cell; T. Bil, total bilirubin; TC, total cholesterol; TP, total protein; WBC, white blood cell.

suggested that no hepatitis virus or nonhepatitis viral infections or autoimmune hepatitis was involved in her liver injury (Table 1). CT showed a decreased liver volume (914 ml) and a relatively diffuse hypodensity of the hepatic parenchyma. These findings suggested the existence of massive liver necrosis. Furthermore, CT revealed significant gallbladder wall thickening, mild pleural effusion, and ascites.

Figure 1 shows the patient's clinical course. She was diagnosed as having hyperacute-type ALF of unknown etiology based on the precoma period of the disease and the initial examinations. Starting on the first day of her transfer to our hospital, artificial liver support therapy, including hemodialysis filtration, continuous hemodiafiltration, and high-volume plasma exchange, had been administered for 9 days. With these treatments, her consciousness gradually improved, and she recovered completely 3 days after the beginning of artificial liver support therapy. The changes in the SWV values during the clinical course are shown in the lowest panel of Figure 1. The ARF imaging was performed every 4 to 6 days, commencing on admission. An Acuson S2000 scanner with a 4.5-MHz convex-type probe (Siemens Medical Solutions, Mountain View, CA) was used. The region of interest was set in the area 2 cm from the surface of liver segment 5, through the intercostal space (Figure 2). The SWV was measured 10 times consecutively. The mean SWV value excluding outliers was regarded as the result of the liver stiffness measurement. The SWV value was 3.4 ± 0.2 m/s on admission; it increased to 3.6 ± 0.3 m/s on the 5th day after admission and improved on the 18th and 39th hospital days (2.3 ± 0.2 m/s and 1.6 ± 0.1 m/s, respectively). Regarding liver func-

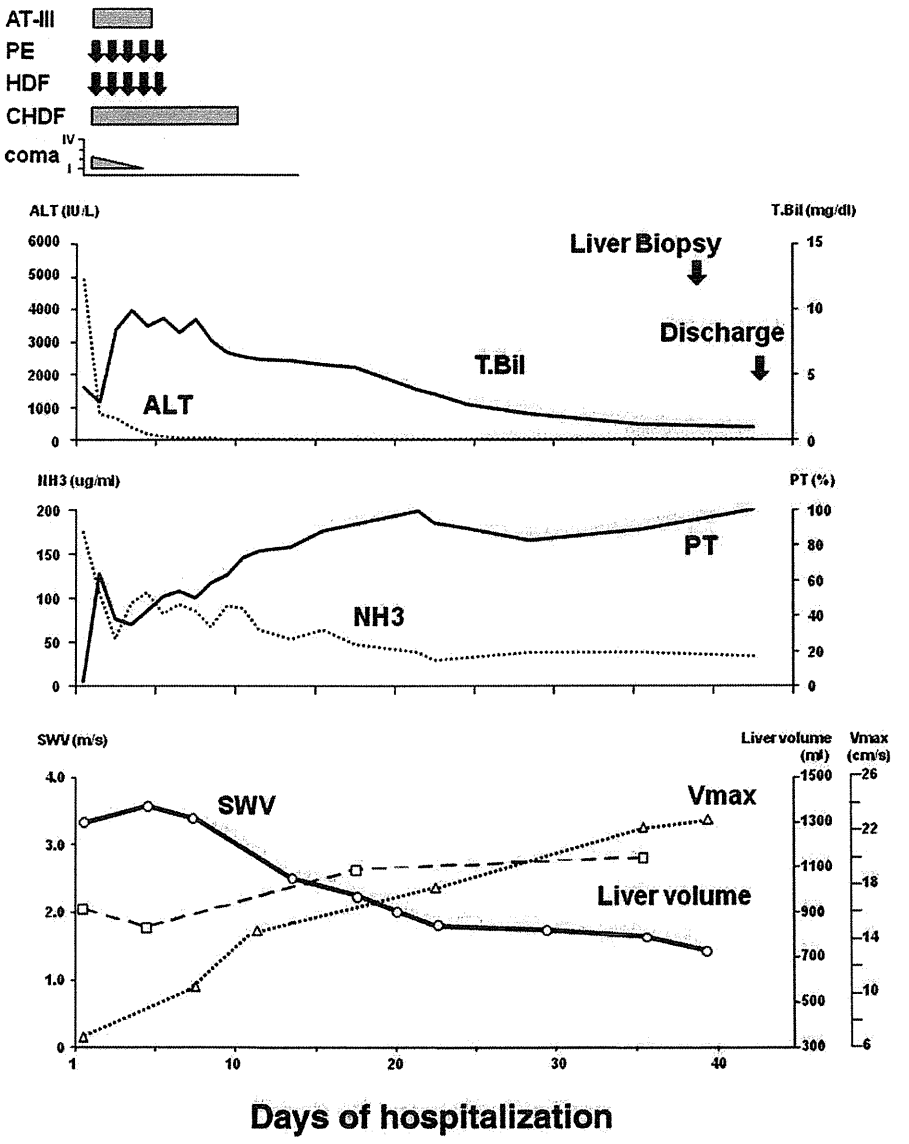

FIGURE 1. The patient's clinical course. SWV, shear wave velocity; Vmax, maximal portal venous velocity; NH3, ammonia; PT, prothrombin time; ALT, alanine transaminase; T.Bil, total bilirubin; AT-III, antithrombin III; PE, plasma exchange; HDF, hemodialysis filtration; CHDF, continuous hemodiafiltration.

tion tests, the serum total bilirubin level increased to 10.2 mg/dl on the third day after admission and then gradually declined. Finally, all of the liver function tests returned to their normal ranges on the 35th day after admission. The liver volume as recorded by CT volumetry decreased to 832 ml on the 5th day after admission, but thereafter recovered to 1090 ml and 1140 ml on the 18th and 36th hospital days, respectively (Figure 3A). The blood flow in the right portal vein measured by pulsed Doppler imaging was decreased to 7.4 cm/s on admission, and then it increased to 16.4, 20, and 25.7 cm/s on the 8th, 22nd, and 36th days after admission, respectively (Figure 3B). The patient underwent an ultrasound-guided liver biopsy using a 14-G biopsy needle on the 39th hospital day and was discharged on the 44th hospital day. The biopsy was performed on liver segment 5, on which the ARFI had been performed. Figure 4 shows the histopathological findings of the biopsy. The portal region had lymphocytic infiltration (Figure 4A). The fibrotic areas extended radially from the portal region toward the direction of the parenchyma, and some bridging fibrosis and pericellular fibrosis was observed (Figure 4B). Although

these findings supported an underlying viral disease, the causal virus was not identified.

DISCUSSION

ARFI is a new technology that insonates tissues with an acoustic push pulse and detects the degree of deformation of the tissue, thereby enabling real-time measurement of liver stiffness.[8,9] The advantage of ARFI technology over TE is that measurements can be performed with software integrated into a conventional ultrasound machine. Thus, the elastography examination can be done in the same session and with the same machine used for the conventional ultrasound examination. Moreover, ARFI can be done in patients with ascites, such as in this case, because the region of interest can be set under real-time ultrasound guidance, which is not possible with TE.

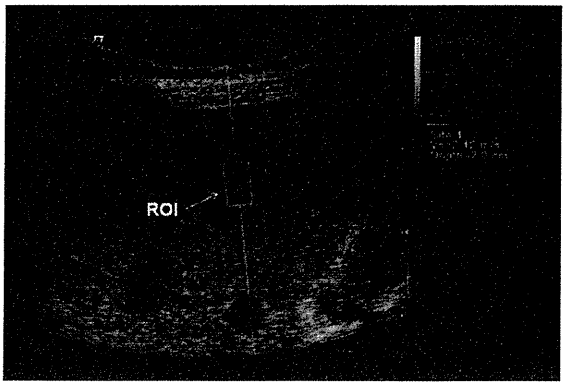

FIGURE 2. Acoustic radiation force impulse (ARFI) imaging on the 20th day of disease. The value of the shear wave velocity is 2.12 m/s. Sonogram shows the placement of the region of interest (arrow) for measurement of shear wave velocity at a depth of 2 cm from the surface of liver in segment 5, through the intercostal space.

Liver elastography using US methods such as TE and ARFI was first developed for the purpose of determining the extent of the fibrosis in chronic liver disease. Several reports have demonstrated that the diagnostic accuracy of SWV measurement using ARFI was comparable to that obtained by TE in the prediction of severe fibrosis and cirrhosis.[10,11,13–15] However, there are no reliable data regarding the clinical role of ARF imaging in patients with ALF. The changes in SWV values of ARFI examinations demonstrated in this case suggest the possibility that the SWV value reflects the severity of liver tissue damage

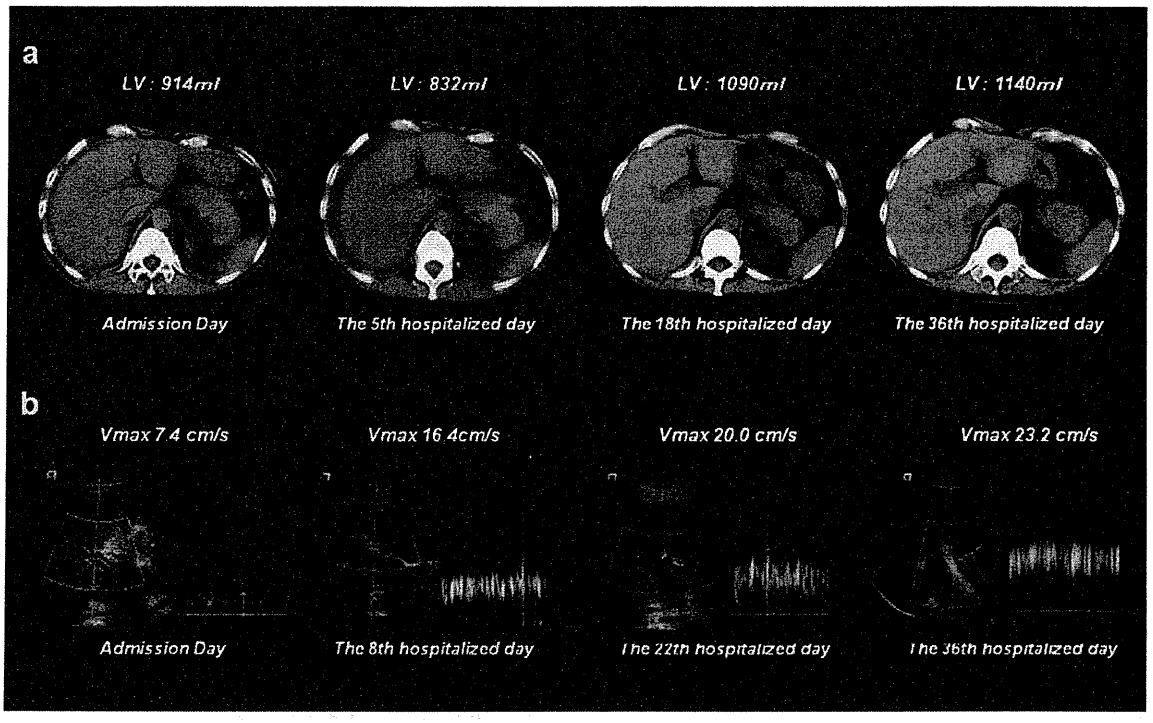

FIGURE 3. The changes in the liver volume and blood flow of the right portal vein during the clinical course. **(A)** The change in liver volume. The liver volume measured by CT was 914 ml on admission day. Although the progression of liver atrophy was seen on the 5th day of disease, with a volume of 832 ml, evidence of recovery was seen on the 18th and 36th days of disease, with volumes of 1090 and 1140 ml, respectively. **(B)** Although the blood flow in the right portal vein was decreased to 7.4 cm/s on the day of admission, it later increased to 16.4, 20, and 25.7 cm/s on the 8th, 22nd, and 36th days of disease, respectively.

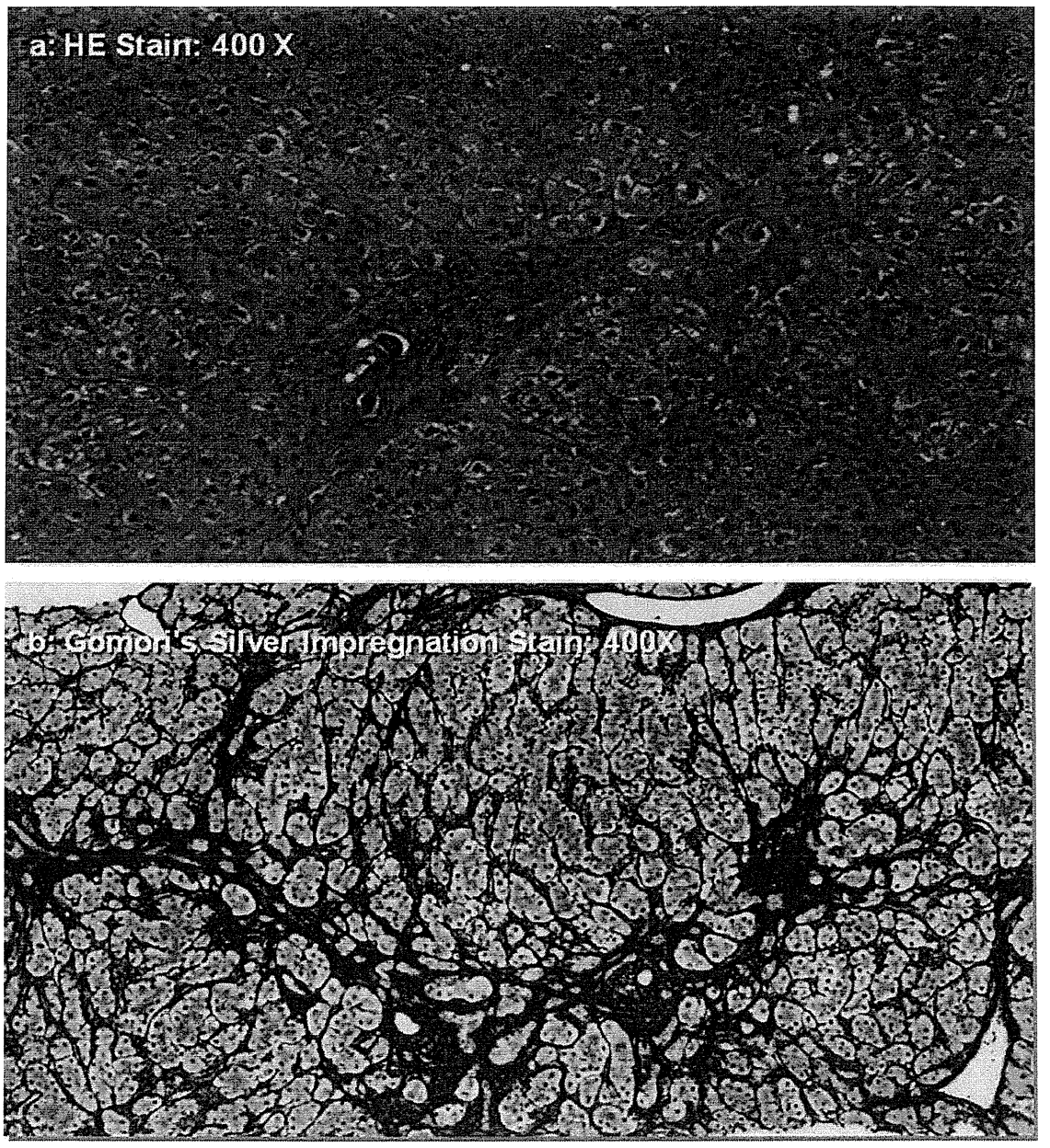

FIGURE 4. Histopathological findings of the liver biopsy performed on the 39th day of hospitalization. **(A)** Hematoxylin and eosin stain (×400). The portal region shows lymphocytic infiltration. **(B)** Gomori's silver impregnation stain (×400) shows some bridging fibrosis and pericellular fibrosis.

in ALF, and therefore, can serve as a biomarker of prognosis and of the necessity for liver transplantation.

The mechanism by which acute hepatic injury increases liver stiffness has not yet been elucidated. Although liver fibrosis is known to be the main factor underlying the increased liver stiffness in chronic liver disease, other histopathological changes were recently reported to be implicated in acute liver injury.[5–7] The histopathological features of ALF are extensive infiltration with inflammatory lymphocytes, along with swelling of hepatocytes and apoptosis without fibrosis. The peak SWV value in the present case was 3.6 ± 0.3 m/s, which was substantially higher than the mean SWV value of 2.3 ± 1.1 m/s in patients with liver cirrhosis type C found in our previous report.[11] These findings suggest that inflamma-

tory changes, other than fibrosis, play an important role in the increase of liver stiffness in ALF.

The establishment of an early and noninvasive method for predicting the prognosis of patients with ALF is urgently needed for determining the necessity for liver transplantation. Therefore, further studies regarding the clinical value of ARFI examination should be undertaken in patients with acute liver injury, including ALF.

REFERENCES

1. Stravitz RT, Kramer AH, Davern T, et al. Acute Liver Failure Study Group: Intensive care of patients with acute liver failure: recommendations of the U.S. Acute Liver Failure Study Group. Crit Care Med 2007;35:2498.
2. Williams R, Wendon J. Indications for orthotopic liver transplantation in fulminant liver failure. Hepatology 1994;20:S5.
3. Donaldson BW, Gopinath R, Wanless IR, et al. The role of transjugular liver biopsy in fulminant liver failure: relation to other prognostic indicators. Hepatology 1993;18:1370.
4. Murakami T, Baron RL, Peterson MS. Liver necrosis and regeneration after fulminant hepatitis: pathological correlation with CT and MR findings. Radiology 1996;198:239.
5. Arena U, Vizzutti F, Corti G, et al. Acute viral hepatitis increases liver stiffness values measured by transient elastography. Hepatology 2008;47:380.
6. Sagir A, Erhardt A, Schmitt M, et al. Transient elastography is unreliable for detection of cirrhosis in patients with acute liver damage. Hepatology 2008;47:592.
7. Cobbold JF, Taylor-Robinson SD. Transient elastography in acute hepatitis: All that's stiff is not fibrosis. Hepatology 2008;47:370.
8. Nightingale K, McAleavey S, Trahey G. Shear-wave generation using acoustic radiation force: in vivo and ex vivo results. Ultrasound Med Biol 2003;29:1715.
9. Fahey BJ, Nightingale KR, Stutz DL, et al. Acoustic radiation force impulse imaging of thermally- and chemically-induced lesions in soft tissues: preliminary ex vivo results. Ultrasound Med Biol 2004;30:321.
10. Lupsor M, Badea R, Stefanescu H, et al. Performance of a new elastographic method (ARFI technology) compared to unidimensional transient elastography in the noninvasive assessment of chronic hepatitis C. Preliminary results. J Gastrointestin Liver Dis 2009;18:303.
11. Friedrich-Rust M, Wunder K, Kriener S, et al. Liver fibrosis in viral hepatitis: noninvasive assessment with acoustic radiation force impulse imaging versus transient elastography. Radiology 2009;252:595.
12. Yoneda M, Suzuki K, Kato S, et al. Nonalcoholic fatty liver disease: US-based acoustic radiation force impulse elastography. Radiology 2010;256:640.
13. Castera L, Forns X, Alberti A. Non-invasive evaluation of liver fibrosis using transient elastography. J Hepatol 2008;48:835.
14. Kuroda H, Kakisaka K, Tatemichi Y, et al. Noninvasive evaluation of liver fibrosis using Acoustic Radiation Force Impulse Imaging in chronic hepatitis patients with hepatitis C virus infection. Hepatogastroenterology 2010;57:1203.
15. Sporea I, Sirli R, Deleanu A, et al. Comparison of the liver stiffness measurement by transient elastography with the liver biopsy. World J Gastroenterol 2008;14:6513.

Non-invasive Markers of Liver Fibrosis

Hidekatsu Kuroda, Yasuhiro Takikawa and Kazuyuki Suzuki

Division of Gastroenterology and Hepatology, Department of Internal Medicine, Iwate Medical University School of Medicine

Abstract

The clinical management and prognosis of chronic liver disease (CLD) are strongly influenced by the extent of liver fibrosis. Although liver biopsy is still considered the gold standard for the staging of liver fibrosis, non-invasive assessment of liver fibrosis has significant advantages for patients with CLD. Non-invasive methods for assessment of liver fibrosis are divided into three markers (serum fibrosis markers, fibrosis scores and imaging technique). Serum fibrosis markers and fibrosis scores are used as non-invasive and quantitative methods to evaluate liver fibrosis. Furthermore, non-invasive measurement methods using imaging techniques such as transient elastography or acoustic radiation force impulse (ARFI) imaging are useful to estimate the degree of fibrosis in CLD. This article reviews the characteristics and the utility of non-invasive serum fibrosis markers and fibrosis scores of liver fibrosis in CLD, and particularly the validity, accuracy and flexibility of ARFI imaging.

Keywords

Liver fibrosis, non-invasive, chronic liver disease, fibrosis marker, fibrosis score, acoustic radiation force impulse imaging

Disclosure: The authors have no conflicts of interest to declare.
Received: 6 November 2011 **Accepted:** 13 December 2011 **Citation:** *European Gastroenterology & Hepatology Review*, 2011;7(4):264–7
Correspondence: Hidekatsu Kuroda, Division of Gastroenterology and Hepatology, Department of Internal Medicine, Iwate Medical University School of Medicine, Uchimaru 19-1, Morioka, Iwate 020-8505, Japan. E: hikuro@iwate-med.ac.jp

In recent years, many methods for non-invasive assessment of liver fibrosis using imaging tests have been developed and implemented in clinical applications. However, because some of these methods are complicated or require expensive equipment, these methods are not yet widely used around the world. It is considered that non-invasive assessment of liver fibrosis provides significant advantages for patients with chronic liver disease (CLD). We reviewed the characteristics and the utility of non-invasive markers of liver fibrosis in CLD, and particularly evaluated the validity, accuracy and flexibility of acoustic radiation force impulse (ARFI) imaging.

The Clinical Impact of Assessment of Liver Fibrosis

Generally, over the course of CLD, liver fibrosis gradually develops and ultimately progresses to cirrhosis. However, because the progression of liver fibrosis does not involve any subjective or objective symptoms, there are occasionally cases that have already developed cirrhosis. In chronic hepatitis C virus (HCV) the progression of liver fibrosis is accompanied by an increase in the hepatic carcinogenesis rate.[1] Moreover, the sustained virological response to interferon therapy, which is the only radical treatment method for CLD related to HCV, decreases as fibrosis develops.[2] However, cases have been observed in which fibrosis is improved as a result of virus removal, not only for chronic hepatitis related to HCV but also for other CLD. These data indicate that the diagnosis of liver fibrosis is very important for assessing disease severity and determining therapeutic strategy.

Methods for Assessment of Liver Fibrosis

Among the means for measuring the grade of liver fibrosis, it has long been the case that histological evaluation of the fibrosis using a liver biopsy is the gold standard.[3] Hepatic tissue images obtained using a liver biopsy are used to semi-quantitatively evaluate the grade of inflammation and the stage of fibrosis. Previously, the histological activity index proposed by Knodeil and revised by Ishak et al. was used, but because this method is somewhat complicated, in recent years, the METAVIR classification proposed by a French group and the new Inuyama classification proposed by a Japanese group are used.[4–6] These classify fibrosis grades using five stages from 0 to 4, and are simple and easy to use. However, there are several problems with histological evaluations based on these liver biopsies. First, liver biopsies involve a sampling error of approximately 25–40 %.[7] This is because tissue obtained through a liver biopsy represents only part of the entire liver, it does not necessarily reflect an overall image of the liver. Furthermore, it has also been reported that the histological diagnoses made by pathologists vary by around 20 %.[8] However, the main reason why liver biopsy is avoided is because it is an invasive procedure. Currently, most liver biopsies are performed using ultrasonic guidance and are relatively safe, but there is a risk of severe complications such as bleeding.[9] Therefore, some patients are unable to undergo this procedure easily, and based on considerations of cost, it is not a procedure that can be performed frequently.

On this basis, attempts have been made to evaluate liver fibrosis without performing a liver biopsy (see *Table 1*). Blood tests are simple and easy to perform, and so various factors have been examined. The factor that has the most impact and is easy to use is platelet count (Plt).[10] However, Plt varies greatly between patients and does not necessarily provide an accurate reflection of liver fibrosis. Fibrosis markers such as type IV collagen 7S, type III procollagen peptide and hyaluronic acid (HA) have been widely used, but reports have